

Analyst

Accepted Manuscript



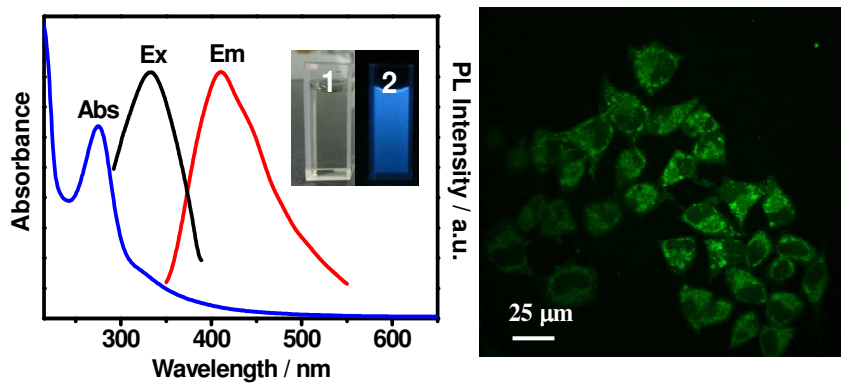
This is an *Accepted Manuscript*, which has been through the Royal Society of Chemistry peer review process and has been accepted for publication.

Accepted Manuscripts are published online shortly after acceptance, before technical editing, formatting and proof reading. Using this free service, authors can make their results available to the community, in citable form, before we publish the edited article. We will replace this *Accepted Manuscript* with the edited and formatted *Advance Article* as soon as it is available.

You can find more information about *Accepted Manuscripts* in the [Information for Authors](#).

Please note that technical editing may introduce minor changes to the text and/or graphics, which may alter content. The journal's standard [Terms & Conditions](#) and the [Ethical guidelines](#) still apply. In no event shall the Royal Society of Chemistry be held responsible for any errors or omissions in this *Accepted Manuscript* or any consequences arising from the use of any information it contains.

Graphical Abstract



A simple and green hydrothermal method was developed for preparation of water-soluble nitrogen-doped carbon dots (N-CDs) from streptomycin. The prepared N-CDs reveal low toxicity, high stability and good biocompatibility, which can be used as fluorescent probes for cell imaging.

Facile synthesis of water-soluble and biocompatible fluorescent nitrogen-doped carbon dots for cell imaging

Weiping Wang, Ya-Chun Lu, Hong Huang, Jiu-Ju Feng,* Jian-Rong Chen, Ai-Jun Wang*

College of Chemistry and Life Science, College of Geography and Environmental Science, Zhejiang Normal University, Jinhua 321004, China

*Corresponding author: Tel./Fax: +86-579-82282269, E-mail: jjfeng@zjnu.cn (JJF); ajwangnju@gmail.com (AJW).

Abstract

A simple, facile and green hydrothermal method was developed in the synthesis of water-soluble nitrogen-doped carbon dots (N-CDs) from streptomycin. The as-prepared N-CDs displayed bright blue fluorescence under the irradiation of UV light, together with a high quantum yield of 7.6% and good biocompatibility as demonstrated by the cell viability assay. Thus, the N-CDs can be used as fluorescent probes for cell imaging, which have potential applications in bioimaging and related fields. This strategy opens a new way for preparation of fluorescent carbon nanomaterials using small molecules as carbon sources.

Keywords: Fluorescence; Nitrogen-doped carbon dots; Streptomycin; Cell imaging

Introduction

Considerable attention has been paid to fluorescent carbon nanomaterials over past several years, owing to their unique physical properties and numerous promising applications in nanobiotechnology. Carbon dots (CDs), as a new member of the carboxylated carbonaceous materials family, have attracted tremendous interest since its discovery.¹ Their unique properties are largely attributed to the large surface area, good biocompatibility, and chemical inertness, as well as unique electronic, optical and thermal characteristics. The CDs have promising potential applications in biological labeling,² bioimaging,³⁻⁶ biosensing,⁷ and optoelectronic devices.^{8,9} Their advantages over other types of semiconductor quantum dots (QDs) are ascribed to their good biocompatibility and low-toxicity.¹⁰⁻¹² Thus, many methods have been developed, which are mainly classified to two types (i.e. top-down and bottom-up synthesis).^{9, 13} Specifically, “top-down” approach is a method of breaking bulk material into small pieces by acid oxidation, electrochemical oxidation, and thermal decomposition.¹⁴⁻¹⁷ Alternatively, “bottom-up” methods include wet-chemical, solvothermal, and microwave-assisted methods, in which the CDs were prepared from molecular precursors under specific reaction conditions.^{9, 18-20}

To improve the solubility and fluorescent properties of the CDs, especially the intrinsic low emission efficiency, several strategies have been designed to extend their applications in biosensing and bioimaging, such as surface passivation and doping with inorganic salts.²⁰⁻²³ For instance, doping with nitrogen is widely used, because nitrogen atom has a comparable atomic size and five valence electrons to bind carbon

atoms.²⁴ Such functionalization can improve the properties of the CDs, as well as extending their potential and/or practical applications.^{20, 25} Zhang et al. prepared nitrogen-doped CDs (N-CDs) from dried monkey grass for the detection of iodide.²⁶ Wu and coworkers fabricated the N-CDs from *Bombyx mori* silk and used as a fluorescent probe in bioimaging.²⁵ Xu' group synthesized multicolor N-CDs using *L*-alanine, *L*-histidine, and *L*-arginine as precursors, and applied to the living cell system.²⁷ However, the complex procedures and strong acid treatment are usually involved.²⁸⁻³⁰

In this work, a simple and facile method was developed for one-step hydrothermal synthesis of fluorescent N-CDs from streptomycin. Their emission property, quantum yield, stability, solubility and toxicity were investigated in some detail.

Experimental

Chemicals

Streptomycin was purchased from Aladdin Ltd. (Shanghai, China). All the other chemicals were of analytical grade and used as received. Twice-distilled water was used for preparation of all aqueous solutions in the whole experiments.

Preparation of the N-CDs

The N-CDs were prepared by hydrothermal treatment of streptomycin (Fig. 1). Typically, 0.1 g streptomycin was dissolved into 35 mL of water under stirring. The

solution was transferred to a 50 mL Teflon-lined autoclave, heated at 200 °C for 12 h, and cooled to room temperature naturally. Next, the aqueous solution was centrifuged at 12000 rpm for 20 min to discard the non-fluorescent deposit, while the N-CDs suspension was kept for further characterization.

Instruments

UV-vis absorption spectra of the samples were recorded on a Lambda 950 UV-vis spectrophotometer (Perkin-Elmer, USA). Fluorescence spectroscopy measurements were conducted on a LS-45 fluorescence spectrophotometer (Perkin-Elmer, UK). Fluorescence lifetime experiments were performed on an Edinburgh FLS 920 photocounting system. X-ray diffraction (XRD) analysis was carried out on a Philips PW3040/60 automatic powder diffractometer using Cu K α radiation. Fourier transform infrared spectroscopy (FT-IR) experiments were conducted on a Nicolet 670 FT-IR spectrometer in the form of KBr pellets. Zeta potentials were measured on a Malvern Zetasizer Nano ZS dynamic light scattering system. The fluorescence images were acquired on a Leica laser confocal fluorescence microscope (TCS SP5).

Cell imaging and Toxicity assay

The cytotoxicity of the N-CDs to human epithelial carcinoma (Hela) cells was evaluated by a standard methylthiazolyldiphenyltetrazolium bromide (MTT) assay. Hela cells were seeded in 96-well U-bottom plates at a density of $5 \times 10^4 \sim 1 \times 10^5$ cells

per milliliter (90 μL per well) that were initially cultured for 12 h in an incubator (37 $^{\circ}\text{C}$, 5% CO_2), followed by the addition of the N-CDs suspension with different concentrations. After another 24 h cultured with the N-CDs, 20 μL of the MTT solution (normal saline or 1 mg mL^{-1} phosphate buffer solution) was added to each sample and incubated at 37 $^{\circ}\text{C}$ for 4 h. The culture media were discarded, followed by the addition of 150 μL of dimethylsulfoxide (DMSO) to dissolve the formazan under shaking for more than 15 min. The corresponding spectra were recorded with a microplate reader at 570 nm. The cell viability rate (VR) was calculated based on the below equation:

$$VR (\%) = A/A_0 \times 100\%$$

Where A is the absorbance of the experimental group (the cells were treated with the N-CDs suspensions) and A_0 is the absorbance of the control group.

Results and discussion

Fig. 2A shows the typical UV-vis absorption spectrum of the as-prepared N-CDs. Clearly, a strong peak is detected at 275 nm, which is attributed to the $\pi-\pi^*$ transition of C=O bond,^{25, 31} revealing the typical absorption of the aromatic π orbitals, which is consistent with that of polycyclic aromatic hydrocarbons.³² The N-CDs suspension displays light yellow (inset 1 in Fig. 2A), which exhibits bright blue fluorescence under the UV light with the excitation of 365 nm (inset 2 in Fig. 2A). Furthermore, the sample shows the maximum emission peak centered at 410 nm, with a full width at half maximum (FWHM) of 94 nm, which is similar to that of the carbon particles

obtained from strawberry juice,³³ but different from that prepared with glycine.³⁴ Meanwhile, with the variation of the excitation wavelength from 333 to 500 nm, the N-CDs emit at longer wavelength (Fig. 2B), displaying tunable emission properties. Therefore, the N-CDs exhibit an excitation-dependent emission, which is an intrinsic property of the carbon particles, as demonstrated by the extensive reports previously.^{23, 35-37}

The fluorescence quantum yield is about 7.6%, using quinine sulfate (54% in 0.1 mol L⁻¹ H₂SO₄, $\lambda_{\text{ex}} = 333$ nm) as a reference. This value is similar to the carbon nanoparticles reported previously,^{4, 14, 38} but larger than those prepared from ascorbic acid,²⁹ glucose and 4,7,10-trioxa-1,13-tridecanediamine.³⁹ This is ascribed to the surface passivation of the CDs in the present work. The fluorescence lifetime is measured to be 7.42 ns, with excitation and emission wavelengths of 333 and 410 nm, respectively (Fig. S1, Supporting Information). This value is higher than those of the carbon nanoparticles reported before.^{4, 25, 40}

Representative TEM image clearly reveals that the N-CDs are nearly spherical with a diameter of 2.97 nm (Fig. 3B). Moreover, high-resolution TEM (HRTEM) image (inset in Fig. 3A) displays the clear lattice fringes with the interfringe distance of 0.202 nm, which is assigned to the (102) planes of graphitic (sp²) carbon.⁴¹ This observation is similar to that fabricated from graphite powder,⁴² but different from that of the carbon nanoparticles synthesized with activated carbon.⁴³

Impressively, the N-CDs show a diffraction peak located at 22.6° in the XRD spectrum (Fig. 4A), suggesting that the interlayer spacing of the (002) diffraction peak

is 0.41 nm, similar to that of the carbon nanoparticles prepared from citric acid with branched polyethylenimine,⁴⁴ but larger than that of graphite (0.34 nm), possibly owing to the existence of oxygen-containing functional groups.⁴⁰

The functional groups of the N-CDs were characterized by FT-IR spectroscopy (Fig. 4B). There is a broad peak at around 3420 cm^{-1} , corresponding to the O-H stretching vibration, indicating the presence of abundant hydroxyl groups. The peak at 1640 cm^{-1} is attributed to the C=O stretching mode. And the peaks at 1400 cm^{-1} and 1100 cm^{-1} come from the C-O-C groups.^{16, 29, 32, 41, 45} These observations demonstrate the coexistence of hydroxyl and carboxylic groups on the surface of the N-CDs, as also supported by the zeta potential experiments with a value of -29.4 mV .^{14, 20}

The surface composition and oxidation states of the N-CDs were examined by XPS measurements. In the survey XPS spectrum, the peaks at 286.1 eV, 402.1 eV, and 532.1 eV (Fig. 5A) correspond to the elements of C_{1s} , N_{1s} , and O_{1s} , respectively. These results indicate that the N-CDs are composed of C, O, and N elements with the percentage of 60.26%, 26.73%, and 9.15%, respectively. The amount of N is smaller than those fabricated from cocoon silk,²⁰ but higher than those prepared from strawberry juice³³ and grass.⁴⁶ It indicates that streptomycin can be used for surface passivation of the CDs. Specifically, the deconvolution of the C_{1s} (Fig. 5B) indicates the existence of $sp^2\text{ C=C}$ (284.8 eV), C-O (286.2 eV), and C=O (287.9 eV) groups. There are two peaks observed at 530.7 eV and 532.0 eV in the O_{1s} spectrum (Fig. 5C), which are assigned to the C=O and C-OH/C-O-C groups, respectively. The N_{1s} spectrum (Fig. 5D) has two peaks at 399.9 eV and 401.4 eV, which are attributed to

the C-N-C and N-(C)₃ groups, respectively.

Herein, a series of control experiments are performed to examine the stability of the N-CDs. As shown in Fig. 6A, the fluorescence intensities are almost unchanged by varying the NaCl concentrations (up to 500 mM), revealing high stability of the N-CDs even under high ionic strength conditions. Similarly, the fluorescence intensity is nearly constant after the sample is treated by 500 W Xe lamp for 6 h (Fig. 6C) or stored for three months (Fig. 6D), while other conditions were kept unchanged. Alternatively, the variation of the pH values from 3 to 10 has slight effects on the fluorescence intensity (Fig. 6B), while the intensity is dropped down as the pH is up to 12. As a result, the N-CDs have good stability over the entire physiologically pH range, enabling them with a wide range of applications, unlike those obtained from polyethylenimine⁴⁷ and citric acid⁴⁸. These results verify the improved stability of the N-CDs, possibly owing to the electrostatic repulsions between the negatively charged nanoparticles. Therefore, the N-CDs are particularly valuable for real applications in bio-labelling and bio-imaging.

To demonstrate the as-prepared N-CDs as fluorescent probes in cell imaging, the MTT assay was carried out, using Hela cell as a model cell (Fig. 7). The N-CDs exhibit fairly low cytotoxicity with cells retaining viability of 100% and 78% at the concentrations of 55 and 825 $\mu\text{g mL}^{-1}$, respectively, suggesting low cytotoxicity and good biocompatibility of the N-CDs, compared with those in the literature.^{13, 39, 49}

Impressively, the N-CDs concentrations are much higher for the *in vitro* evaluation, compared with those required for potential applications such as optical

imaging of living cells.⁵⁰ Similarly, the exposure time under UV light is much longer than routine use. It means that the N-CDs possess chemical inertness and almost no cytotoxicity even in harsh environments.

Importantly, the N-CDs uptake and bioimaging experiments were also performed by the confocal fluorescence microscope *in vitro*. As illustrated in Fig. 8, the morphologies of the Hela cells are almost unchanged before (Fig. 8A) and after (Fig. 8C) incubation with the N-CDs, further confirming their good biocompatibility and low toxicity. The bright green areas inside the Hela cells are clearly observed by exciting at 488 nm (Fig. 8D), while it's hard to distinguish fluorescent area under bright field (Fig. 8B). These results suggest good stability of the N-CDs. Notably, the fluorescent spots are observed only in the cytoplasm, while very weak fluorescence intensity is detected at the central region, indicating that the N-CDs are easy to penetrate into the cells but only in the cytoplasm. This observation is consistent with the previous studies on the interactions of living cells with nanomaterials,^{2, 51, 52} in which genetic disruption do not occur.⁵⁰ All these results demonstrate very good biocompatibility of the N-CDs, which can be used as an excellent optical probe for cell imaging.

Conclusion

In summary, a simple, facile, efficient and green method was developed for preparation of the fluorescent N-CDs using streptomycin as carbon sources. The as-synthesized water-soluble N-CDs showed bright and stable blue fluorescence,

which were closely dependent on the excitation wavelength. The N-CDs have tunable emission properties, excellent stability and low cytotoxicity. These advantages make the N-CDs as a promising imaging agent in bioimaging, protein analysis and cells tracking. This strategy may open a new route for constructing other functional carbon nanomaterials as highly specific catalysts and drug targeting carriers.

Acknowledgements

This work was financially supported by the NSFC (Nos. 21175118, 21275130, 21275131, 21305128 and 21345006), and Zhejiang province university young academic leaders of academic climbing project (No. pd2013055).

References

1. X. Xu, R. Ray, Y. Gu, H. J. Ploehn, L. Gearheart, K. Raker and W. A. Scrivens, *J. Am. Chem. Soc.*, 2004, **126**, 12736-12737.
2. M. Zhang, L. Bai, W. Shang, W. Xie, H. Ma, Y. Fu, D. Fang, H. Sun, L. Fan, M. Han, C. Liu and S. Yang, *J. Mater. Chem.*, 2012, **22**, 7461-7467.
3. S. Zhuo, M. Shao and S.-T. Lee, *ACS Nano*, 2012, **6**, 1059-1064.
4. J. Zhou, Z. Sheng, H. Han, M. Zou and C. Li, *Mater. Lett.*, 2012, **66**, 222-224.
5. C. Yu, X. Li, F. Zeng, F. Zheng and S. Wu, *Chem. Commun.*, 2013, **49**, 403-405.
6. P.-C. Hsu, P.-C. Chen, C.-M. Ou, H.-Y. Chang and H.-T. Chang, *J. Mater. Chem. B*, 2013, **1**, 1774-1781.
7. S. Zhu, Q. Meng, L. Wang, J. Zhang, Y. Song, H. Jin, K. Zhang, H. Sun, H. Wang

- and B. Yang, *Angew. Chem.*, 2013, **125**, 4045-4049.
8. C. Zhu, J. Zhai and S. Dong, *Chem. Commun.*, 2012, **48**, 9367-9369.
 9. J. Shen, Y. Zhu, X. Yang and C. Li, *Chem. Commun.*, 2012, **48**, 3686-3699.
 10. L. Zhou, Z. Li, Z. Liu, J. Ren and X. Qu, *Langmuir*, 2013, **29**, 6396-6403.
 11. S.-T. Yang, L. Cao, P. G. Luo, F. Lu, X. Wang, H. Wang, M. J. Meziani, Y. Liu, G. Qi and Y.-P. Sun, *J. Am. Chem. Soc.*, 2009, **131**, 11308-11309.
 12. X. Wang, K. Qu, B. Xu, J. Ren and X. Qu, *Nano Res.*, 2011, **4**, 908-920.
 13. Z. Qian, J. Ma, X. Shan, L. Shao, J. Zhou, J. Chen and H. Feng, *RSC Adv.*, 2013, **3**, 14571-14579.
 14. H. Yan, M. Tan, D. Zhang, F. Cheng, H. Wu, M. Fan, X. Ma and J. Wang, *Talanta*, 2013, **108**, 59-65.
 15. H. Li, X. He, Z. Kang, H. Huang, Y. Liu, J. Liu, S. Lian, C. H. A. Tsang, X. Yang and S.-T. Lee, *Angew. Chem. Int. Ed.*, 2010, **49**, 4430-4434.
 16. Y. Dong, H. Pang, S. Ren, C. Chen, Y. Chi and T. Yu, *Carbon*, 2013, **64**, 245-251.
 17. Y. Dong, N. Zhou, X. Lin, J. Lin, Y. Chi and G. Chen, *Chem. Mater.*, 2010, **22**, 5895-5899.
 18. Y. Yang, D. Wu, S. Han, P. Hu and R. Liu, *Chem. Commun.*, 2013, **49**, 4920-4922.
 19. Y. N. Tan, J. Y. Lee and D. I. C. Wang, *J. Am. Chem. Soc.*, 2010, **132**, 5677-5686.
 20. W. Li, Z. Zhang, B. Kong, S. Feng, J. Wang, L. Wang, J. Yang, F. Zhang, P. Wu and D. Zhao, *Angew. Chem. Int. Ed.*, 2013, **52**, 1-6.

21. F. L. Braghiroli, V. Fierro, M. T. Izquierdo, J. Parmentier, A. Pizzi and A. Celzard, *Carbon*, 2012, **50**, 5411-5420.
22. P. Wu and X.-P. Yan, *Chem. Soc. Rev.*, 2013, **42**, 5489-5521.
23. J. Shen, Y. Zhu, X. Yang, J. Zong, J. Zhang and C. Li, *New J. Chem.*, 2012, **36**, 97-101.
24. Y. Li, Y. Zhao, H. Cheng, Y. Hu, G. Shi, L. Dai and L. Qu, *J. Am. Chem. Soc.*, 2011, **134**, 15-18.
25. Z. L. Wu, P. Zhang, M. X. Gao, C. F. Liu, W. Wang, F. Leng and C. Z. Huang, *J. Mater. Chem. B*, 2013, **1**, 2868-2873.
26. H. Zhang, Y. Li, X. Liu, P. Liu, Y. Wang, T. An, H. Yang, D. Jing and H. Zhao, *Environ. Sci. Technol. Lett.*, 2013, DOI:10.1021/ez400137j.
27. Y. Xu, M. Wu, Y. Liu, X.-Z. Feng, X.-B. Yin, X.-W. He and Y.-K. Zhang, *Chem. Eur. J.*, 2013, **19**, 2276-2283.
28. M. Tan, L. Zhang, R. Tang, X. Song, Y. Li, H. Wu, Y. Wang, G. Lv, W. Liu and X. Ma, *Talanta*, 2013, **115**, 950-956.
29. X. Jia, J. Li and E. Wang, *Nanoscale*, 2012, **4**, 5572-5575.
30. S. Liu, L. Wang, J. Tian, J. Zhai, Y. Luo, W. Lu and X. Sun, *RSC Adv.*, 2011, **1**, 951-953.
31. A. Sachdev, I. Matai, S. U. Kumar, B. Bhushan, P. Dubey and P. Gopinath, *RSC Adv.*, 2013, **3**, 16958-16961.
32. R. Liu, H. Li, W. Kong, J. Liu, Y. Liu, C. Tong, X. Zhang and Z. Kang, *Mater. Res. Bull.*, 2013, **48**, 2529-2534.

33. H. Huang, J.-J. Lv, D.-L. Zhou, N. Bao, Y. Xu, A.-J. Wang and J.-J. Feng, *RSC Adv.*, 2013, **3**, 21691-21696.
34. P.-C. Hsu and H.-T. Chang, *Chem. Commun.*, 2012, **48**, 3984-3986.
35. J. Zhou, Y. Yang and C.-y. Zhang, *Chem. Commun.*, 2013, **49**, 8605-8607.
36. Y.-P. Sun, B. Zhou, Y. Lin, W. Wang, K. A. S. Fernando, P. Pathak, M. J. Meziani, B. A. Harruff, X. Wang, H. Wang, P. G. Luo, H. Yang, M. E. Kose, B. Chen, L. M. Veca and S.-Y. Xie, *J. Am. Chem. Soc.*, 2006, **128**, 7756-7757.
37. H. Peng and J. Travas-Sejdic, *Chem. Mater.*, 2009, **21**, 5563-5565.
38. J. Wei, J. Shen, X. Zhang, S. Guo, J. Pan, X. Hou, H. Zhang, L. Wang and B. Feng, *RSC Adv.*, 2013, **3**, 13119-13122.
39. Y. Song, W. Shi, W. Chen, X. Li and H. Ma, *J. Mater. Chem.*, 2012, **22**, 12568-12573.
40. J. Peng, W. Gao, B. K. Gupta, Z. Liu, R. Romero-Aburto, L. Ge, L. Song, L. B. Alemany, X. Zhan, G. Gao, S. A. Vithayathil, B. A. Kaiparettu, A. A. Marti, T. Hayashi, J.-J. Zhu and P. M. Ajayan, *Nano Lett.*, 2012, **12**, 844-849.
41. W. Lu, X. Qin, S. Liu, G. Chang, Y. Zhang, Y. Luo, A. M. Asiri, A. O. Al-Youbi and X. Sun, *Anal. Chem.*, 2012, **84**, 5351-5357.
42. S.-L. Hu, K.-Y. Niu, J. Sun, J. Yang, N.-Q. Zhao and X.-W. Du, *J. Mater. Chem.*, 2009, **19**, 484-488.
43. Y. Dong, C. Chen, J. Lin, N. Zhou, Y. Chi and G. Chen, *Carbon*, 2013, **56**, 12-17.
44. Y. Dong, R. Wang, H. Li, J. Shao, Y. Chi, X. Lin and G. Chen, *Carbon*, 2012, **50**, 2810-2815.

45. H. Zhu, X. Wang, Y. Li, Z. Wang, F. Yang and X. Yang, *Chem. Commun.*, 2009, 5118-5120.
46. S. Liu, J. Tian, L. Wang, Y. Zhang, X. Qin, Y. Luo, A. M. Asiri, A. O. Al-Youbi and X. Sun, *Adv. Mater.*, 2012, **24**, 2037-2041.
47. L. Shen, L. Zhang, M. Chen, X. Chen and J. Wang, *Carbon*, 2013, **55**, 343-349.
48. W. Shi, X. Li and H. Ma, *Angew. Chem.*, 2012, **124**, 6538-6541.
49. L. Shang, R. M. Dorlich, S. Brandholt, R. Schneider, V. Trouillet, M. Bruns, D. Gerthsen and G. U. Nienhaus, *Nanoscale*, 2011, **3**, 2009-2014.
50. F. Wang, Z. Xie, H. Zhang, C.-y. Liu and Y.-g. Zhang, *Adv. Funct. Mater.*, 2011, **21**, 1027-1031.
51. X. Zhai, P. Zhang, C. Liu, T. Bai, W. Li, L. Dai and W. Liu, *Chem. Commun.*, 2012, **48**, 7955-7957.
52. Y. Xu, M. Wu, X.-Z. Feng, X.-B. Yin, X.-W. He and Y.-K. Zhang, *Chem. Eur. J.*, 2013, **19**, 6282-6288.

Captions

Fig. 1. Chemical structure of streptomycin.

Fig. 2. (A) UV-vis absorption spectrum (blue), photoluminescence excitation (black), and emission (red) spectra of the N-CDs in aqueous solutions. (B) The corresponding emission spectra by varying the excitation wavelengths from 333 to 500 nm with 20 nm increment. Insets show the corresponding photographs under visible light (1) and UV light (2), respectively.

Fig. 3. TEM image (A) and the particle size distribution (B) of the N-CDs. Inset shows the high magnification TEM image of a nitrogen-doped carbon dot.

Fig. 4. XRD pattern (A) and FT-IR spectrum (B) of the N-CDs.

Fig. 5. XPS survey (A), and high-resolution C_{1s} (B), O_{1s} (C) and N_{1s} (D) spectra of the N-CDs.

Fig. 6. Effects of the NaCl concentrations (A), pH values from 3 to 12 (B), time intervals of irradiation with a 500 W Xe lamp (C), and storage time (D) on the fluorescence intensity of the N-CDs.

Fig. 7. Cell viability assays of the cells treated with different concentrations of the N-CDs.

Fig. 8. Images of Hela cells in the absence (A, B) and presence (C, D) of the CDs obtained under bright field (A, C) and by excitation at 488 nm (B, D). The concentration of the CDs is $55 \mu\text{g mL}^{-1}$.

Figures

Fig. 1

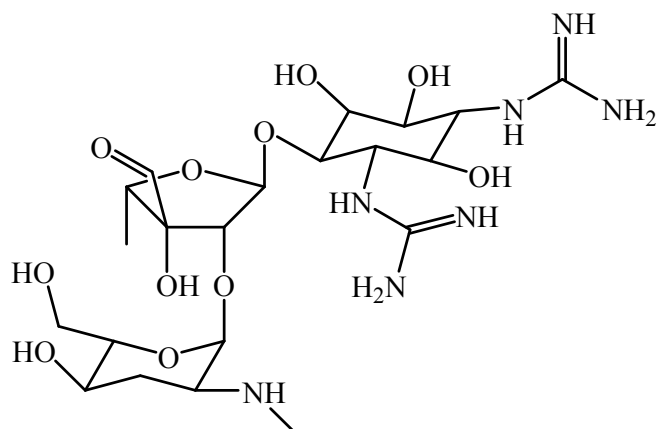


Fig. 2

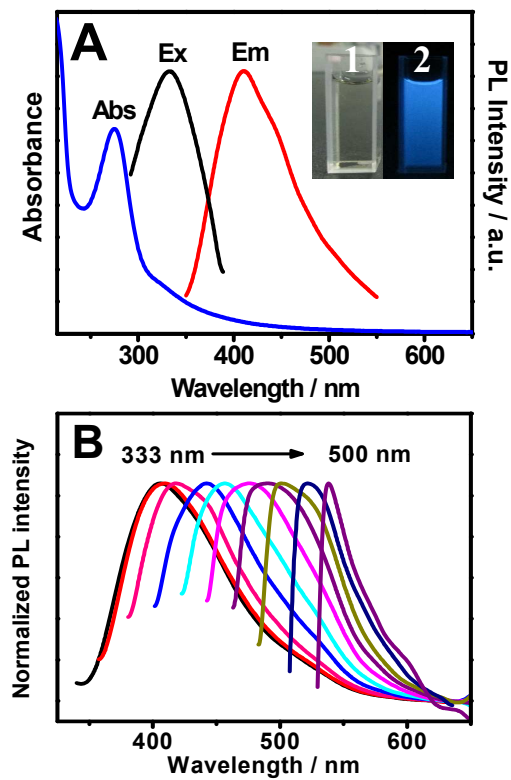


Fig. 3

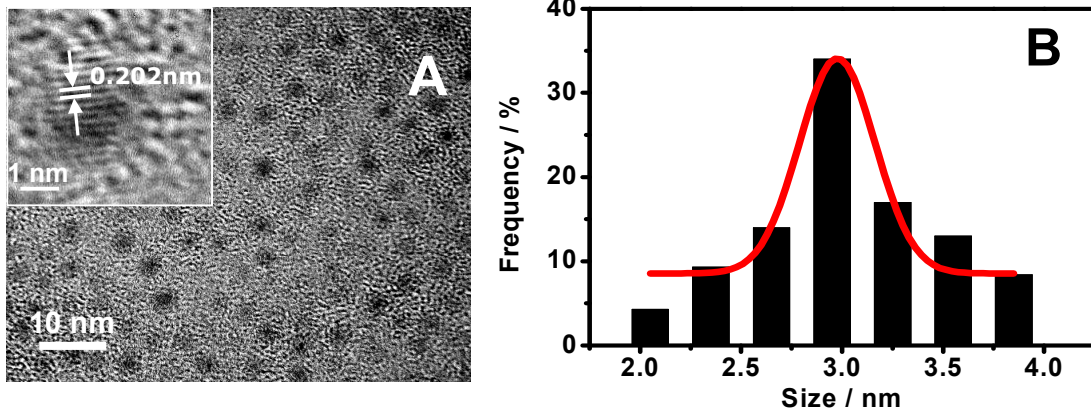


Fig. 4

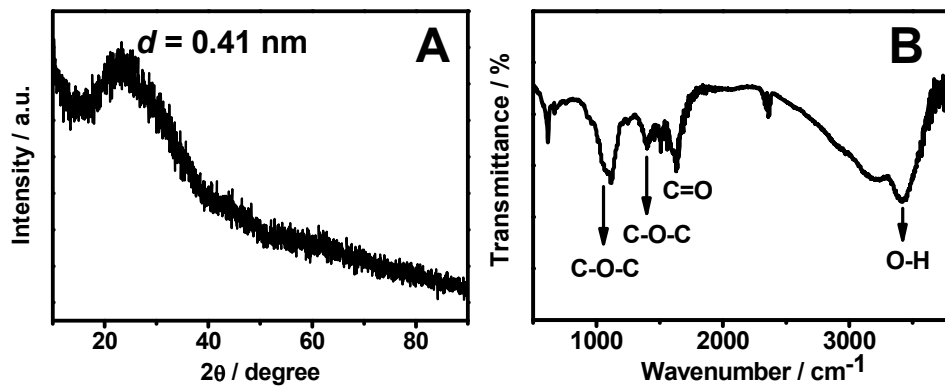


Fig. 5

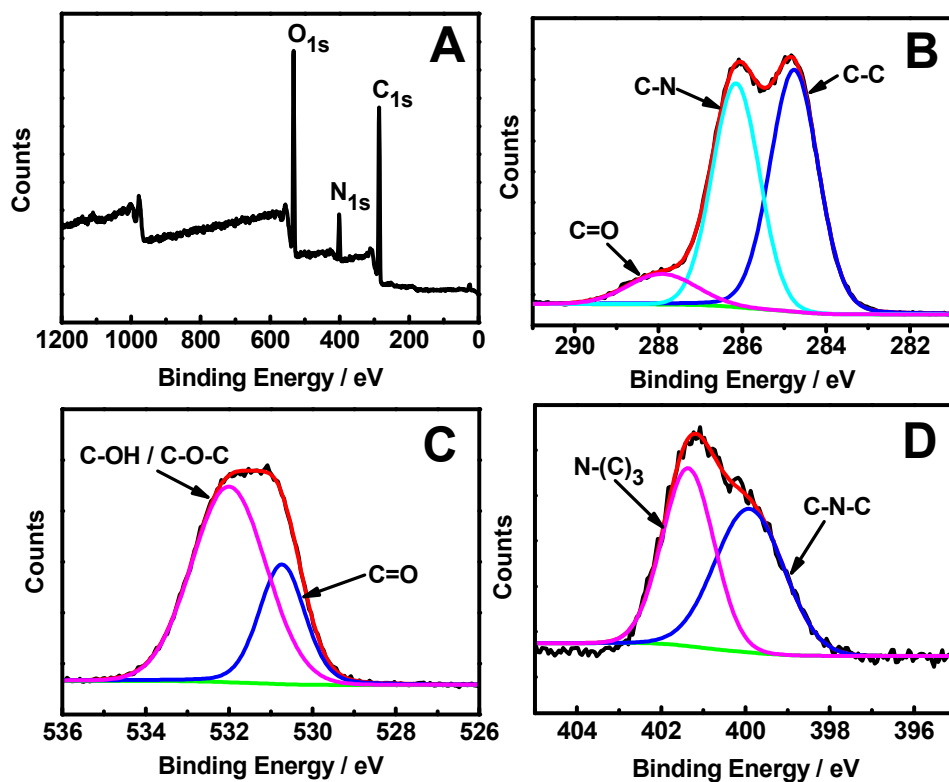


Fig. 6

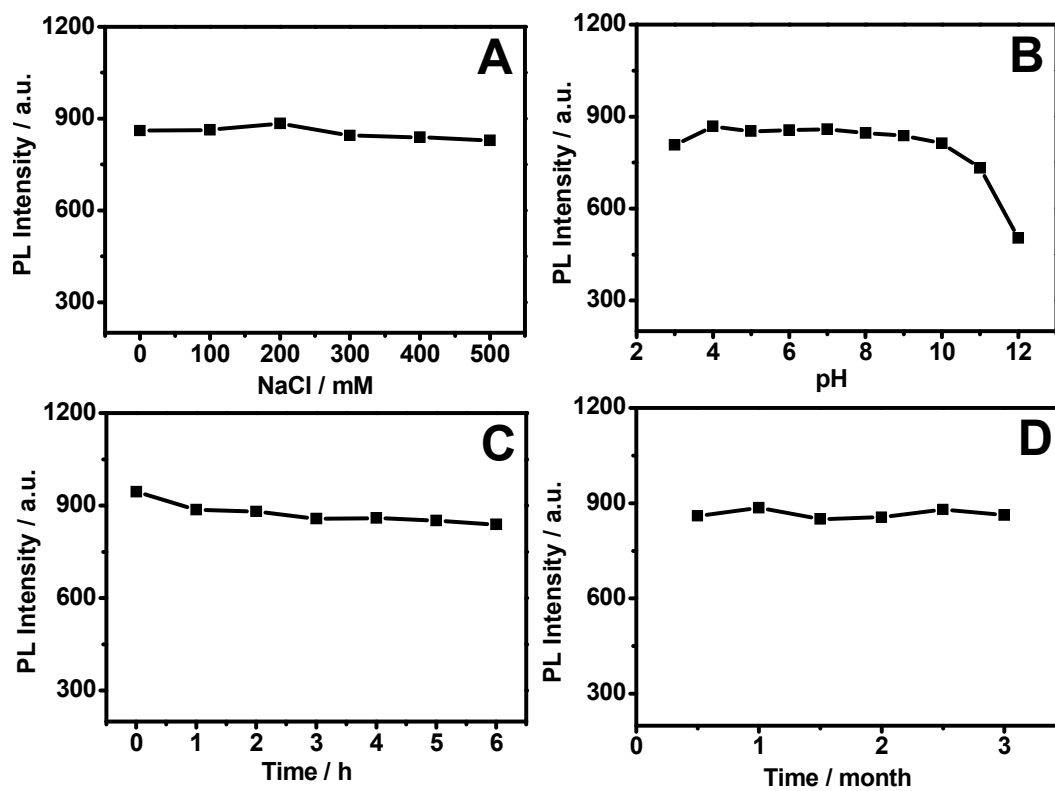


Fig. 7

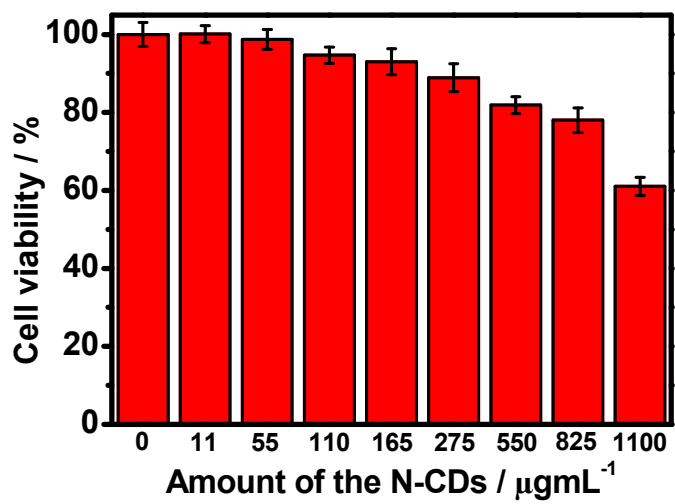


Fig. 8

